nature

# EMBRYONIC STEM CELLS

Proven reprogramming of primate skin cells

STELLAR EVOLUTION
A new shade of white dwarf

RISING OR FOE?
Scientists know the score

LIFESPAN EXTENSION
Surprise activity of an antiaging enzyme

NATURE JOBS
Research in India

ARTICLES

# Producing primate embryonic stem cells by somatic cell nuclear transfer

J. A. Byrne[1]†, D. A. Pedersen[1], L. L. Clepper[1], M. Nelson[3], W. G. Sanger[3], S. Gokhale[3], D. P. Wolf[1] & S. M. Mitalipov[1,2]

**Derivation of embryonic stem (ES) cells genetically identical to a patient by somatic cell nuclear transfer (SCNT) holds the potential to cure or alleviate the symptoms of many degenerative diseases while circumventing concerns regarding rejection by the host immune system. However, the concept has only been achieved in the mouse, whereas inefficient reprogramming and poor embryonic development characterizes the results obtained in primates. Here, we used a modified SCNT approach to produce rhesus macaque blastocysts from adult skin fibroblasts, and successfully isolated two ES cell lines from these embryos. DNA analysis confirmed that nuclear DNA was identical to donor somatic cells and that mitochondrial DNA originated from oocytes. Both cell lines exhibited normal ES cell morphology, expressed key stem-cell markers, were transcriptionally similar to control ES cells and differentiated into multiple cell types *in vitro* and *in vivo*. Our results represent successful nuclear reprogramming of adult somatic cells into pluripotent ES cells and demonstrate proof-of-concept for therapeutic cloning in primates.**

ES cells can differentiate into multiple cell types, representatives of which could be used in replacement therapy for ageing or diseased cells and tissues[1]. However, ES cells derived from *in vitro* fertilized (IVF) embryos are genetically divergent from the patient (allogenic) and thus any resultant transplanted cell would be rejected without the continual application of immunosuppressive drugs[2]. One way to resolve completely the transplant rejection issue would be to generate ES cells that are genetically identical to the patient. Recent reports suggest that somatic cells can be directly reprogrammed into ES-cell-like cells in mice, after transfection with key stem-cell-specific (stemness) genes[3–5]. However, the ability to extrapolate this approach to other mammals, including primates, remains in question, and the propensity of such cells to develop into tumours owing to *c-myc* transgene reactivation remains a concern[4]. Alternatively, ES cells can be derived by epigenetic reprogramming of somatic cells via SCNT in spindle-free oocytes, a process commonly referred to as therapeutic cloning (Supplementary Fig. 1). However, despite encouraging results in the murine model[6,7], the feasibility of therapeutic cloning in primates remains in question. Although many mammals have been successfully produced by means of SCNT[8] no successful primate reproductive cloning has been achieved[9,10]. Moreover, the efficiency of blastocyst formation after human[11] and non-human primate[9] SCNT has typically been very low, suggesting lack or incomplete nuclear reprogramming with existing SCNT protocols. We recently reported incomplete nuclear remodelling, including nuclear envelope breakdown and premature chromosome condensation, after standard SCNT in rhesus macaques (*Macaca mulatta*) and correlated this observation with a decline in maturation promoting factor activity[12]. SCNT protocols designed to prevent premature cytoplast activation and maturation promoting factor decline resulted in robust nuclear envelope breakdown and premature chromosome condensation and in significantly increased blastocyst development, suggesting that maturation promoting factor activity is instrumental for efficient nuclear reprogramming[12]. Here we used these SCNT protocols to demonstrate therapeutic cloning in the rhesus macaque and provide a translational model for testing the feasibility, therapeutic effectiveness and long-term safety of therapeutic cloning as a concept.

## Embryo development and ES cell derivation

The primary culture of skin fibroblasts, used as the source of nuclear donor cells for SCNT, was established from a nine-year-old adult rhesus macaque male (male 1) housed at the Oregon National Primate Research Center (Supplementary Fig. 2). Mature metaphase II rhesus macaque oocytes were rendered spindle-free with the Oosight spindle imaging system that uses polarized light to visualize the oocyte meiotic spindle (Supplementary Fig. 3). Analysis of the removed karyoplasts, for the presence of the meiotic spindles, consistently confirmed a 100% efficiency of spindle removal using this approach. The donor fibroblast nuclei were introduced into cytoplasts by electrofusion, incubated for 2 h to allow nuclear remodelling to occur, and subsequently activated and cultured to the blastocyst stage as described previously[12] (see also Methods). We observed a 16% (35 out of 213) blastocyst formation rate with this nuclear donor cell line (Supplementary Table 1). SCNT blastocysts demonstrated a similar morphology to low-grade IVF blastocysts (Supplementary Fig. 4). Twenty expanded or hatching SCNT blastocysts were used for ES cell derivation via mechanical inner cell mass (ICM) isolation ($n = 2$), immunosurgery ($n = 15$) or direct culture of intact blastocysts ($n = 3$) on mouse embryonic fibroblast (MEF) feeder layers. Two ES cell lines (cloned rhesus embryonic stem: CRES-1 and CRES-2) were derived, both after immunosurgery (10% derivation efficiency from blastocysts). Overall, 304 oocytes collected from 14 rhesus macaque females were used to generate two ES cell lines, a 0.7% derivation efficiency from oocytes.

## Genetic analysis and pluripotency

As the number of mitochondria, each with 16.6 kilobases (kb) of mitochondrial DNA[13] (mtDNA), in the cytoplast dwarfs any mitochondrial contribution from the donor somatic cells, embryos

[1]Oregon National Primate Research Center and [2]Oregon Stem Cell Center, Oregon Health & Science University, 505 N.W. 185th Avenue, Beaverton, Oregon 97006, USA. [3]Munroe-Meyer Institute, 985450 Nebraska Medical Center, Omaha, Nebraska 68198, USA. [4]Whitehead Institute for Biomedical Research, 9 Cambridge Center, Cambridge, Massachusetts 02142, USA. †Present address: Stanford Institute for Stem Cell Biology and Regenerative Medicine, Stanford University, Palo Alto, California 94304, USA.

derived by SCNT should predominantly, if not exclusively, possess mitochondria inherited from the oocyte[14]. Therefore, ES cells derived from SCNT embryos should contain mtDNA identical to the female providing the recipient cytoplasts and nuclear DNA genetically identical to the male providing the nuclear donor cells. To investigate whether the CRES-1 and CRES-2 cell lines contained the same nuclear DNA as the donor (male 1) fibroblasts, we performed microsatellite typing using 39 short tandem repeat (STR) loci[15] and analysis of 56 single nucleotide polymorphisms (SNPs)[16], 30 of which were informative for inheritance. Both the STR analysis—which included 25 common STR loci (Table 1) and 14 major histocompatibility complex (MHC)-linked STRs (Supplementary Table 2)—and the SNP analysis (Supplementary Table 3) demonstrated a complete match of both CRES lines to each other and to the nuclear DNA isolated from skin fibroblasts and peripheral blood leucocytes of male 1. In contrast, DNA obtained from the oocyte donor females for CRES-1 (female 1) and CRES-2 (female 2) demonstrated no significant similarity to CRES-1 or CRES-2 (Table 1 and Supplementary Tables 2 and 3). The genomic constitution of an IVF-derived rhesus macaque ES cell line (ORMES-22; ref. 17), and the ORMES-22 oocyte donor female (female 3) and sperm donor male (male 2), were also included to demonstrate STR allele inheritance (Table 1 and Supplementary Table 2).

To investigate whether the CRES-1 and CRES-2 cell lines contained the same mtDNA as their respective oocyte donor females, we performed mtDNA sequence analysis investigating an informative domain 1 (ID1) in the rhesus macaque mitochondrial D-loop hypervariable region 2 (RhDHV2). This RhDHV2 sequence contained multiple informative SNPs including at ID1 nucleotide positions 4, 22 and 28 (Fig. 1). Analysis of SNP22 (an A-to-G polymorphism) demonstrated that CRES-1 mtDNA was derived from the oocyte donor female 1 and not from the nuclear donor for CRES-1. Similarly, analysis of SNP4 (a C-to-T polymorphism) and SNP28 (an A-to-G polymorphism) confirmed that the CRES-2 mtDNA was derived from the CRES-2 oocyte donor female 2 and not from the nuclear donor. Thus, microsatellite, SNP and mtDNA analyses verified that CRES-1 and CRES-2 contained nuclear DNA genetically identical to the nuclear donor fibroblasts and mtDNA inherited from oocytes, a hallmark of SCNT-produced ES cells and offspring.

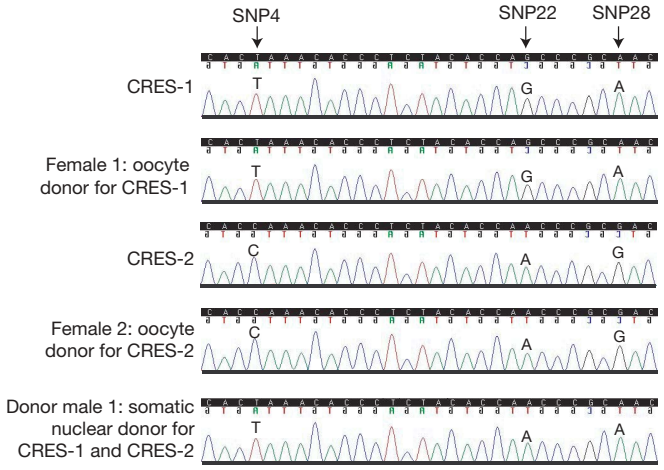


**Figure 1 | Chromatograms of the rhesus macaque mitochondrial D-loop hypervariable region 2 informative domain 1 (RhDHV2 ID1).** The ID1 sequence encompassed *Macaca mulatta* mtDNA nucleotide positions 451–480 (GenBank accession number NC_005943). Sequence analysis revealed that SNP22 (A-to-G) was informative for the mitochondrial inheritance for CRES-1 whereas SNP4 (C-to-T) and SNP28 (A-to-G) were informative for the mitochondrial inheritance for CRES-2. Results were confirmed by three independent sequences.

Both CRES lines demonstrated typical ES cell morphology (Fig. 2a–d), maintained an undifferentiated morphology after repeated manual passaging (>20 passages per line so far) and expressed key primate stemness markers including OCT4 (also called POU5F1), SSEA-4, TRA1-60 and TRA1-81 (Fig. 2). Moreover, transcripts of other stemness genes including *NANOG*, *SOX2*, *LEFTYA* (also called *LEFTY2*), *TDGF* and *TERT* were detected by polymerase chain reaction with reverse transcription (RT–PCR) analysis in both IVF-derived ES cell controls (ORMES-10 and ORMES-22) and CRES cell lines (Supplementary Fig. 5). Conventional cytogenetic G-banding

**Table 1 | Short tandem repeat (STR) analysis of CRES cell lines**

| STR loci | Female 1 oocyte donor for CRES-1 | Female 2 oocyte donor for CRES-2 | Male 1 somatic nuclear donor for CRES-1 and CRES-2 | CRES-1 | CRES-2 | Female 3 oocyte donor for ORMES-22 | Male 2 sperm donor for ORMES-22 | ORMES-22 |
|---|---|---|---|---|---|---|---|---|
| Sex (AME) | XX | XX | XY | XY | XY | XX | XY | XX |
| D1S548 | 190/206 | 190/198 | 190/190 | 190/190 | 190/190 | 190/190 | 190/190 | 190/190 |
| D2S1333 | 301/301 | 293/301 | 289/301 | 289/301 | 289/301 | 273/293 | 285/289 | 273/285 |
| D3S1768 | 221/221 | 205/213 | 193/217 | 193/217 | 193/217 | 205/213 | 205/205 | 205/205 |
| D4S2365 | 283/283 | 275/287 | 283/283 | 283/283 | 283/283 | 283/283 | 283/283 | 283/283 |
| D4S413 | 131/131 | 133/145 | 131/139 | 131/139 | 131/139 | 131/145 | 125/141 | 131/141 |
| D5S1457 | 136/136 | 132/136 | 132/136 | 132/136 | 132/136 | 132/136 | 132/140 | 136/140 |
| D6S501 | 176/180 | 176/180 | 176/180 | 176/180 | 176/180 | 188/192 | 180/180 | 180/188 |
| D7S513 | 191/205 | 205/209 | 189/191 | 189/191 | 189/191 | 189/217 | 193/199 | 199/217 |
| D7S794 | 108/124 | 124/128 | 128/128 | 128/128 | 128/128 | 108/108 | 108/128 | 108/128 |
| D8S1106 | 144/144 | 148/160 | 144/148 | 144/148 | 144/148 | 148/168 | 160/168 | 168/168 |
| D9S921 | 183/195 | 183/191 | 179/179 | 179/179 | 179/179 | 183/195 | 175/195 | 183/195 |
| D10S1412 | 157/166 | 160/160 | 157/157 | 157/157 | 157/157 | 157/157 | 160/160 | 157/160 |
| D11S2002 | 256/256 | 256/256 | 260/264 | 260/264 | 260/264 | 252/252 | 256/260 | 252/256 |
| D11S925 | 308/338 | 310/316 | 308/310 | 308/310 | 308/310 | 308/308 | 338/338 | 308/338 |
| D12S364 | 282/290 | 282/288 | 281/290 | 281/290 | 281/290 | 282/290 | 268/296 | 268/290 |
| D12S67 | 121/129 | 192/204 | 117/125 | 117/125 | 117/125 | 117/133 | 109/117 | 109/133 |
| D13S765 | 228/240 | 212/220 | 228/256 | 228/256 | 228/256 | 216/236 | 228/228 | 228/236 |
| D15S823 | 333/349 | 329/353 | 329/361 | 329/361 | 329/361 | 357/385 | 345/353 | 345/385 |
| D16S403 | 164/168 | 156/158 | 158/164 | 158/164 | 158/164 | 152/164 | 152/152 | 152/164 |
| D17S1300 | 232/280 | 244/280 | 272/276 | 272/276 | 272/276 | 248/252 | 228/284 | 252/284 |
| D18S537 | 178/178 | 178/178 | 174/178 | 174/178 | 174/178 | 174/178 | 162/174 | 162/178 |
| D18S72 | 306/308 | 306/322 | 306/308 | 306/308 | 306/308 | 308/308 | 306/308 | 308/308 |
| D22S685 | 315/319 | 291/303 | 315/327 | 315/327 | 315/327 | 311/311 | 327/327 | 311/327 |
| MFGT21 | 113/115 | 117/119 | 115/115 | 115/115 | 115/115 | 111/113 | 115/125 | 113/125 |
| MFGT22 | 104/104 | 104/104 | 100/104 | 100/104 | 100/104 | 100/104 | 104/110 | 104/104 |

CRES-1 is an ES cell line isolated from a SCNT blastocyst produced by fusion of a cytoplast donated by female 1 and a skin fibroblast originated from male 1. Similarly, CRES-2 was derived from a cytoplast donated by female 2 and a donor somatic nucleus from male 1. ORMES-22 is an ES cell line derived from an embryo produced by IVF of a female 3 oocyte with a male 2 sperm. AME, amelogenin.

analysis of the nuclear donor fibroblasts used for SCNT (Supplementary Fig. 6) and the CRES-2 cell line (Fig. 3a) demonstrated a normal male rhesus macaque chromosome (42, XY) complement in all cells analysed. However, analysis of the CRES-1 cell line indicated the presence of three metaphase cells representing a hypodiploid clone characterized by loss of the Y chromosome (Supplementary Fig. 7), and seventeen cells representing a diploid clone characterized by an isochromosome comprised of two copies of the long arm of the Y chromosome (41,X[3]/42,X,i(Y)q10)[17]) (Fig. 3b). Subsequent fluorescent *in situ* hybridization (FISH) analysis confirmed the G-banding findings; metaphase cells revealed the presence of a signal for bacterial artificial chromosome (BAC) CH250-283K14 on both arms of the Y chromosome (Fig. 3d), indicating the presence of the i(Y)(q10) observed in the G-banding study. Additional studies were positive for loss of the Y chromosome in 12% of the CRES-1 cells analysed.

### Transcriptional profiling

Global transcription profiles of three biological replicates each of male 1 skin fibroblasts (nuclear donor for both CRES lines), both CRES-1 and CRES-2 cell lines and two control ES cell lines derived from fertilized embryos (ORMES-10 and ORMES-22[17]) were examined by Affymetrix microarray analysis. For the primary microarray comparison (Supplementary Data 3), three types of analyses were performed: (1) replicates of each cell line were compared against each other, (2) each cell line was compared against the somatic donor cell line; and (3) each cell line was compared to a control IVF-derived ES cell line (see Methods). For each comparison, the detected signal for each present 'P' probe set ($P < 0.05$) was plotted in a scatter graph, the number of present probe sets (PP) used was recorded and the correlation value was calculated. All comparisons of control ORMES biological replicates with each other demonstrated a correlation value of greater than 60% and all unrelated sample comparisons (that is, between ES cell and somatic cell biological replicates) demonstrated a correlation value of significantly less than 60%; therefore a correlation value of 60% or greater was considered indicative of a significant transcriptional correlation. When the replicates of the somatic donor cells were compared, 99% transcriptional correlation was observed (Supplementary Fig. 8a), suggesting that minimal artificial variation was introduced via the protocols used. Although it was not possible to determine with certainty the degree of technical versus biological variation between replicates, it should be noted that all samples were processed identically and at the same time, and the level of technical variation between the donor somatic cell samples was 1% or less, suggesting that most of the 20–30% transcriptional variation observed between ES cell replicates was biological in origin. If so, ES cells show significant transcriptional plasticity not observed in somatic cells (Supplementary Fig. 8a). However, further transcriptional profiling will be required to confirm this observation. Comparisons of the CRES cell lines to the somatic donor cells and control IVF-derived ES cells demonstrated that both CRES lines had fully reprogrammed into an ES cell transcriptional state, with no significant transcriptional correlation between the CRES lines and the donor somatic cells (Supplementary Fig. 8b) but a significant

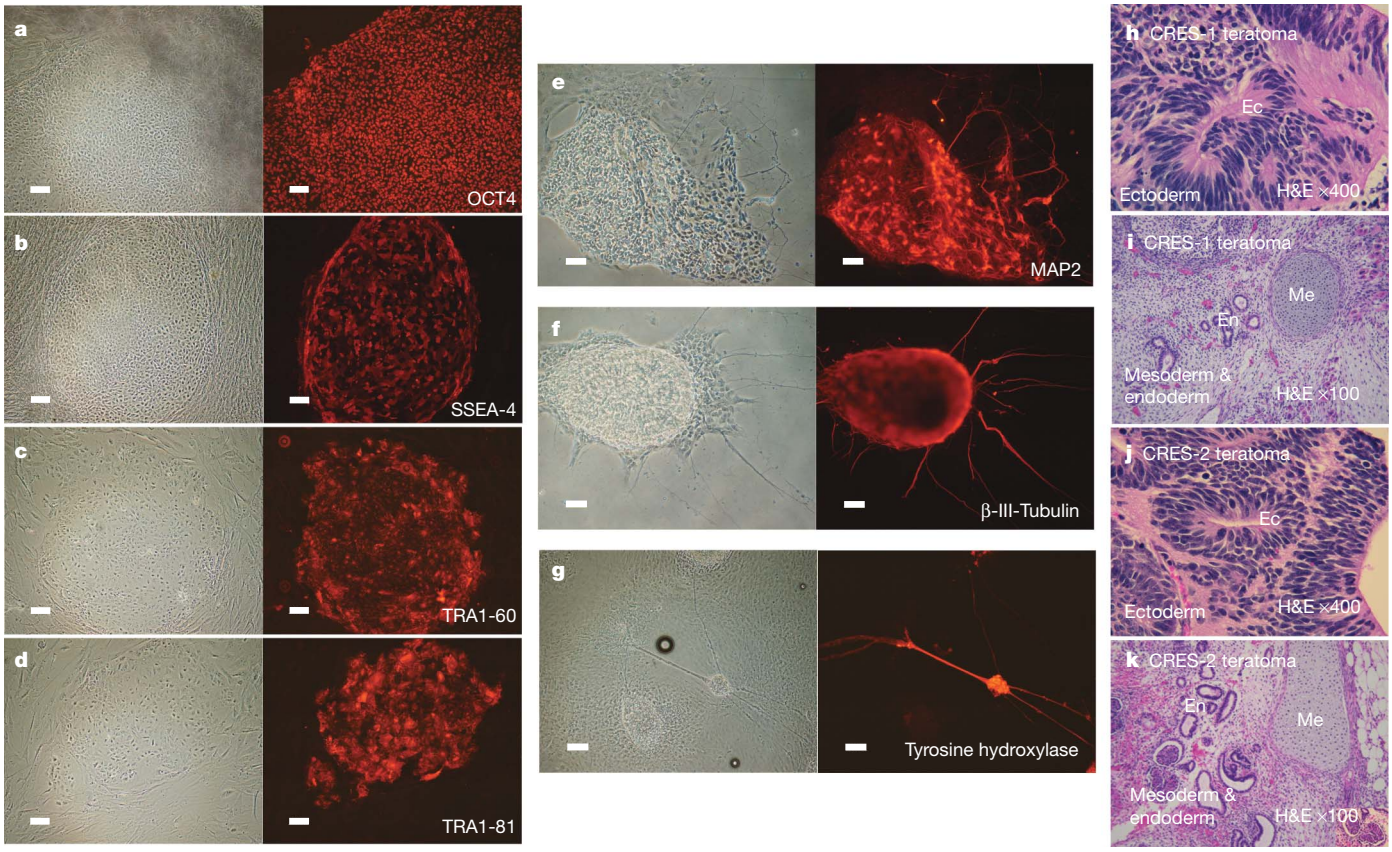


**Figure 2 | Morphological and immunocytochemical analysis of CRES cells and their differentiated derivatives. a–d**, Morphology of CRES colonies and expression of primate ES-cell-specific markers: OCT4, SSEA-4, TRA1-60 and TRA1-81. For each stemness marker analysed, a positive signal was only observed in CRES colonies, not in mouse embryonic fibroblast feeder cells, demonstrating antibody specificity. **e–g**, Cellular morphology and expression of neural markers in differentiated CRES cells, including microtubule-associated protein 2 (MAP2), β-III-tubulin and tyrosine hydroxylase. The left hand column of **a–g** represents phase contrast images and the right hand column demonstrates marker expression as detected via immunocytochemistry. The scale bars in **a–d, g** represent 100 μm and the scale bars in **e**, **f** represent 50 μm. **h**, **j**, Presence of ectoderm (Ec)-derived neuroepithelium (×400, haematoxylin and eosin (H&E)) in teratomas produced by injection of CRES-1 and CRES-2 into SCID mice. **i**, **k**, Presence of mesoderm (Me)-derived cartilage and endoderm (En)-derived glandular epithelium (×100, H&E) in CRES-1 and CRES-2 teratomas.

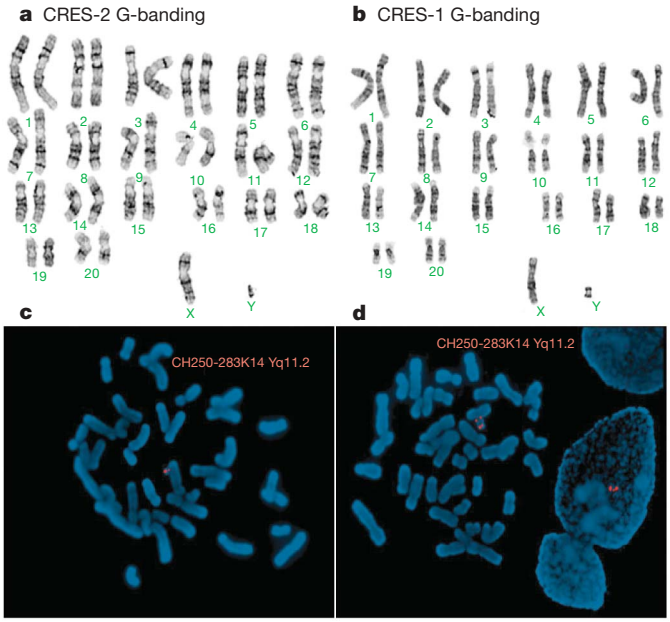


**Figure 3 | Cytogenetic analysis of CRES cells. a**, G-banding of CRES-2 cells demonstrating a normal euploid rhesus karyotype (42, XY). **b**, CRES-1 cell line with aneuploid karyotype, characterized by an isochromosome comprised of two copies of the long arm of the Y chromosome (41,X[3]/42,X,i(Y)q10)[17]). **c**, FISH analysis of the nuclear donor fibroblasts demonstrating a normal karyotype with two red fluorescent signals on the long (q) arm of the Y chromosome. **d**, FISH analysis of CRES-1 cells indicating the presence of four signals for the Y chromosome long (q) arm, confirming the presence of the i(Y)(q10) aneuploidy.

correlation between CRES cells and the control ES cells (Supplementary Fig. 8c).

To identify ES-cell-specific genes, comparison analysis was performed between each of the three control ORMES-10 replicates and each of the three somatic donor cell replicates, to give a total of nine ES cell–somatic comparisons (Supplementary Data 4). This set of ES cell comparisons identified 4,998 somatic-cell-specific probe sets/genes (Supplementary Data 5) and 6,178 ES-cell-specific probe sets/genes (Supplementary Data 6 and Methods). Over 90% of the somatic-cell-specific genes were significantly downregulated in the CRES cell line replicates (Supplementary Table 4), and over 85% of the ES-cell-specific genes demonstrated significantly greater expression in the CRES cell line replicates (Table 2) when compared with the somatic donor cells. Transcriptional analysis of the control ORMES-22 replicates also demonstrated that over 90% of the somatic-specific genes had significantly less expression (Supplementary Table 4) and over 85% of the ES-cell-specific genes had significantly greater expression (Table 2) when compared with the somatic donor cells.

The final microarray analysis involved examining the level of expression of 12 putative rhesus macaque stemness genes identified in previous transcriptional profiling[18]. These putative stemness genes had the highest average fold change in gene expression when undifferentiated ES cell biological replicates were compared to their *in vitro* differentiated counterparts, and all 12 were significantly upregulated in the five different ES cell lines examined[18]. All 12 stemness genes were significantly upregulated in all of the ORMES-10, ORMES-22, CRES-1 and CRES-2 replicates (Supplementary Data 7), and the average fold change in gene expression for both CRES-1 and CRES-2 was comparable to that for ORMES-10 and ORMES-22 when compared to somatic donor cell replicates (Table 3). As a control, the relative fold change in expression for these putative stemness genes between the donor somatic cell replicates was insignificant (Table 3).

Our overall conclusion after analysis of global transcriptional profiles is that both CRES-1 and CRES-2 cells are transcriptionally similar to control ES cell lines derived from IVF-produced blastocysts.

## Differentiation potential

To define pluripotency further, both CRES lines were exposed to conditions for cardiomyocyte differentiation *in vitro*[17]. CRES-1 and CRES-2 efficiently produced contracting aggregates (Supplementary Video) expressing markers of cardiac muscle tissue (Supplementary Fig. 9). Directed neural differentiation resulted in efficient formation of various neural phenotypes, demonstrating elongated cellular morphology and expression of neural markers, including microtubule-associated protein 2 (MAP2; Fig. 2e), β-III-tubulin (Fig. 2f) and tyrosine hydroxylase (Fig. 2g). When injected into severe combined immune deficiency (SCID) mice, both CRES lines formed teratomas and subsequent histological analysis identified representatives of all three germ layers (Fig. 2h–k), confirming their pluripotent status.

## Discussion

Our results demonstrate successful reprogramming of primate somatic cells into pluripotent ES cells, provided that an efficient SCNT method is available. We achieved a significant increase in the blastocyst formation rate (from 1% to 16%) when the use of Hoechst 33342 was avoided during the oocyte spindle removal step. The detrimental effect of fluorochrome bisbenzimide (Hoechst 33342) and ultraviolet light on cytoplast quality has been previously documented[12,19], and we speculate that the impaired blastocyst formation rate after conventional SCNT in primates may result from one or more of the following factors: Hoechst 33342 and/or ultraviolet damage to the relatively transparent primate oocyte; Hoechst 33342/UV-induced oocyte activation and/or maturation promoting factor degradation; reaction of the residual Hoechst 33342 in cytoplasts with the

**Table 2 | Analysis of ES-cell-specific gene expression in rhesus macaque stem cell lines**

| Cell line | Biological replicate | Number of ES cell genes* upregulated compared to donor line replicate A† | Number of ES cell genes* upregulated compared to donor line replicate B† | Number of ES cell genes* upregulated compared to donor line replicate C† |
|---|---|---|---|---|
| Nuclear donor cells | A | N/A | 21 (0.3%) | 47 (0.8%) |
| Nuclear donor cells | B | 30 (0.5%) | N/A | 77 (1.2%) |
| Nuclear donor cells | C | 18 (0.3%) | 13 (0.2%) | N/A |
| ORMES-22 | A | 5,482 (89%) | 5,388 (87%) | 5,389 (87%) |
| ORMES-22 | B | 5,558 (90%) | 5,607 (91%) | 5,644 (91%) |
| ORMES-22 | C | 5,766 (93%) | 5,672 (92%) | 5,723 (93%) |
| CRES-1 | A | 5,974 (97%) | 6,001 (97%) | 5,984 (97%) |
| CRES-1 | B | 5,896 (95%) | 5,919 (96%) | 5,926 (96%) |
| CRES-1 | C | 5,748 (93%) | 5,845 (95%) | 5,784 (94%) |
| CRES-2 | A | 5,931 (96%) | 5,843 (95%) | 5,850 (95%) |
| CRES-2 | B | 5,658 (92%) | 5,552 (90%) | 5,483 (89%) |
| CRES-2 | C | 5,863 (95%) | 5,933 (96%) | 5,889 (95%) |

* The general approximation when working with large numbers of probe sets is to assume that each probe set represents hybridization to a single gene. However, multiple probe sets can exist for certain genes, so the actual number of genes included in the analysis is significantly lower than the number of probe sets analysed.
† The percentage value represents the proportion of probe sets, out of the 6,178 ES-cell-specific probe sets, significantly upregulated after comparison analysis.

**Table 3 | Expression analysis of putative rhesus macaque stemness genes**

| Affymetrix probe set ID | Stemness gene* | Nuclear donor cells fold change† | ORMES-10 fold change† | ORMES-22 fold change† | CRES-1 fold change† | CRES-2 fold change† |
|---|---|---|---|---|---|---|
| MmugDNA.26523.1.S1_s_at | *NFE2L3* | 1 | 429 | 389 | 532 | 378 |
| MmuSTS.2285.1.S1_at | *POU5F1* (*OCT4*) | 0 | 315 | 288 | 320 | 281 |
| MmugDNA.9427.1.S1_at | *NR5A2* | 1 | 282 | 310 | 278 | 325 |
| MmugDNA.32128.1.S1_at | *NANOG* | 1 | 246 | 180 | 256 | 190 |
| MmuSTS.1436.1.S1_at | *LCK* | 1 | 179 | 206 | 218 | 94 |
| MmugDNA.11728.1.S1_at | *VTCN1* | 1 | 245 | 139 | 153 | 125 |
| MmugDNA.42677.1.S1_at | *DPPA4* | 4 | 154 | 117 | 178 | 78 |
| MmugDNA.28461.1.S1_at | *SLC12A1* | 1 | 71 | 128 | 185 | 169 |
| MmugDNA.6836.1.S1_at | *C14orf115* (LOS699513) | 1 | 81 | 87 | 85 | 64 |
| MmuSTS.3122.1.S1_at | *MYRIP* | 0 | 71 | 51 | 75 | 53 |
| MmugDNA.15193.1.S1_at | *ADH4* | 0 | 68 | 13 | 52 | 58 |
| MmuSTS.2310.1.S1_at | *PRDM14* | 1 | 28 | 44 | 46 | 40 |

* The stemness genes were identified in previous transcriptional profiling of rhesus macaque ES cell lines[18]. These 12 genes had the highest average fold change in gene expression of five different rhesus macaque ES cell lines.

† Microarray suite-5 (MAS-5) statistical analysis was performed to calculate the signal log ratio (SLR) for each cell line in comparison to the somatic donor cell line biological replicates, and the averaged gene expression fold change between compared samples was calculated from the SLR using the formula: fold change = ($2^{SLR}$). All 12 stemness genes were significantly upregulated ($P < 0.002$) in CRES cell lines.

introduced donor cell DNA, thereby impairing reprogramming; and/or Hoechst 33342 contact with mitochondrial DNA, thus reducing cytoplast mitochondrial function.

Recognizing the importance of high-quality cytoplasts for successful reprogramming, we have sought non-invasive approaches for spindle detection and removal. 'Blind' enucleation techniques involving 'squish'[20] or 'one-step manipulation'[21] were inefficient, at least in our hands, because they failed to enucleate all oocytes. In fact, our initial effort to derive ES cells from SCNT blastocysts produced with these protocols resulted in the isolation of parthenogenetic ES cells owing to failed spindle removal. Fortunately, recent developments in high-performance imaging resulted in an Oosight spindle imaging system supporting rapid and highly efficient real-time enucleation of primate oocytes. Introduction of the donor nucleus can be accomplished by either direct injection or electrofusion—the latter was dictated here by the relatively large donor cells used. The SCNT blastocyst development rate was significantly lower than fertilized controls but within the 7–29% range described by us when fetal fibroblasts, adult ear fibroblasts, cumulus and oviductal epithelial cells were used as nuclear donor cells in the monkey[12]. Blastocysts produced by SCNT usually demonstrated poor morphology and have, so far, failed to support a term pregnancy after embryo transfer despite considerable efforts[21,22] (D.P.W., unpublished data). This result may not be predictive for ES cell isolation, however, as the requirements for reproductive and therapeutic cloning are different in that a normal trophectoderm is not required for the latter[23].

With an adequate supply of SCNT blastocysts, the final challenge in therapeutic cloning is ES cell isolation, and although several methods were examined, the conventional method involving immunosurgical dispersal of the trophectoderm seemed to be the best. The derivation efficiency in the present study is within the range reported in the mouse, where the ES cell derivation efficiency from SCNT embryos was 0.2–3.4% per oocyte and 4–10% per blastocyst[6,24–27].

Regarding the origin of the CRES lines, in addition to the 100% spindle removal efficiency, karyotype, microsatellite and SNP analyses confirmed that both CRES lines originated from SCNT embryos and not from parthenotes. CRES lines demonstrated typical ES cell morphology, self-renewal capacity and expression of stemness markers. These cell lines were also transcriptionally similar to ES cells derived from fertilized blastocysts, and pluripotent, as demonstrated by the generation of representatives of all three germ layers after *in vivo* teratoma formation. Our results parallel findings in the mouse[28,29] and confirm the possibility of complete nuclear reprogramming of somatic cells into pluripotent ES cells via SCNT. The CRES-1 cell line revealed a translocation of unknown origin characterized by an isochromosome comprised of two copies of the long arm of chromosome Y, whereas CRES-2 exhibited a normal euploid male karyotype. In our previous study[21], five out of seven analysed SCNT blastocysts were karyotypically normal with two embryos demonstrating aneuploidy. Karyotyping individual SCNT embryos based on either biopsied blastomere or trophectodermal cell analysis followed by ES cell isolation could address whether chromosomal abnormalities in SCNT-derived ES cells originate from aneuploid embryos or occur during ES cell isolation and culture.

The primary rationale for therapeutic cloning is transplantation of histocompatible ES-cell-derived phenotypes back into the patient. The MHC profile of both CRES lines perfectly matched the donor male in all MHC loci examined via microsatellite analysis, suggesting that transplantation of differentiated derivatives back into the donor animal would not lead to rejection. It is possible that immune response will occur in the donor animal resulting from the epitopes derived from the allogenic recipient oocyte mitochondria contribution; although preliminary research with cloned bovine and porcine cells and tissues with allogenic mtDNA suggests that grafting back into the nuclear donor organism can occur without destruction by the immune system[30,31]. The use of biological materials from other species, such as fetal bovine serum, mouse embryonic fibroblasts and guinea-pig complement, may also contaminate ES cells with xenoepitopes and pathogens that would make such cells unsuitable for clinical applications. Other possibly minor factors that should nevertheless also be investigated include the problems that may arise from the lack of sperm-derived centrosomes, the possible effects of non-random X-inactivation and the possibility that cloned ES cells may possess the shortened telomeres of their donor somatic cell source. The possibility has also been suggested that SCNT embryos are epigenetically abnormal based on DNA methylation patterns[32]. Therefore, the epigenetic status of CRES cell lines including imprinted gene expression would also be an interesting area for future research.

Assuming that our modified SCNT protocols are applicable to humans, the low efficiency of ES cell derivation (0.7%) along with restricted availability and high cost of human oocytes suggest that a significant increase in the overall SCNT embryo generation and ES cell derivation rates would be required before a clinical implementation of human therapeutic cloning could occur. Recently, mouse ES cells were relatively efficiently cloned using aged, failed-to-fertilize oocytes[33], and substantial numbers of such human oocytes augmented by immature oocytes are routinely discarded, representing an untested source for human SCNT. In addition to therapeutic cloning, human SCNT-derived ES cells would also be extremely valuable in studies devoted to understanding disease mechanisms and developing possible treatments through *in vitro* experimentation[34].

## METHODS SUMMARY

A primary culture of fibroblasts was established from a skin biopsy of an adult rhesus macaque male (male 1) and prepared for SCNT as previously described[9]. Mature metaphase II oocytes were rendered spindle-free using the Oosight imaging system (CRI, Inc.) and a donor somatic cell nucleus was introduced

into a cytoplast through electrofusion. Reconstructed embryos were activated 2 h after fusion by exposure to 5 μM ionomycin (CalBiochem) for 5 min followed by a 5-h incubation in 2 mM 6-dimethylaminopurine (DMAP), placed in HECM-9 medium and cultured at 37 °C in 6% $CO_2$, 5% $O_2$ and 89% $N_2$ until the expanded blastocyst stage. The ICMs of selected SCNT blastocysts were plated onto MEF feeder layers and cultured in ES cell culture medium for 5–7 days. ICMs that attached to the feeder layer and initiated outgrowth were manually dissociated into small clumps with a microscalpel and replated onto fresh MEFs. After the first passage, colonies with ES-cell-like morphology were selected for further propagation, characterization, low-temperature storage and *in vitro* and *in vivo* differentiation, as previously described[17].

**Full Methods** and any associated references are available in the online version of the paper at www.nature.com/nature.

**Received 24 May; accepted 9 October 2007.**


1. McKay, R. Stem cells–hype and hope. *Nature* **406,** 361–364 (2000).
2. Drukker, M. & Benvenisty, N. The immunogenicity of human embryonic stem-derived cells. *Trends Biotechnol.* **22,** 136–141 (2004).
3. Takahashi, K. & Yamanaka, S. Induction of pluripotent stem cells from mouse embryonic and adult fibroblast cultures by defined factors. *Cell* 126, 663–676 (2006); published online 10 August 2006.
4. Okita, K., Ichisaka, T. & Yamanaka, S. Generation of germline-competent induced pluripotent stem cells. *Nature* 448, 313–317 (2007); published online 6 June 2007.
5. Wernig, M. *et al. In vitro* reprogramming of fibroblasts into a pluripotent ES-cell-like state. *Nature* 448, 318–324 (2007); published online 6 June 2007.
6. Rideout, W. M. III, Hochedlinger, K., Kyba, M., Daley, G. Q. & Jaenisch, R. Correction of a genetic defect by nuclear transplantation and combined cell and gene therapy. *Cell* **109,** 17–27 (2002).
7. Barberi, T. *et al.* Neural subtype specification of fertilization and nuclear transfer embryonic stem cells and application in parkinsonian mice. *Nature Biotechnol.* **21,** 1200–1207 (2003).
8. Wilmut, I. *et al.* Somatic cell nuclear transfer. *Nature* **419,** 583–586 (2002).
9. Mitalipov, S. M., Yeoman, R. R., Nusser, K. D. & Wolf, D. P. Rhesus monkey embryos produced by nuclear transfer from embryonic blastomeres or somatic cells. *Biol. Reprod.* **66,** 1367–1373 (2002).
10. Simerly, C. *et al.* Molecular correlates of primate nuclear transfer failures. *Science* **300,** 297 (2003).
11. Hall, V. J. *et al.* Developmental competence of human *in vitro* aged oocytes as host cells for nuclear transfer. *Hum. Reprod.* **22,** 52–62 (2007).
12. Mitalipov, S. M. *et al.* Reprogramming following somatic cell nuclear transfer in primates is dependent upon nuclear remodeling. *Hum. Reprod.* **22,** 2232–2242 (2007).
13. Birky, C. W. Jr. Uniparental inheritance of mitochondrial and chloroplast genes: mechanisms and evolution. *Proc. Natl Acad. Sci. USA* **92,** 11331–11338 (1995).
14. Bowles, E. J., Campbell, K. H. & St John, J. C. Nuclear transfer: preservation of a nuclear genome at the expense of its associated mtDNA genome(s). *Curr. Top. Dev. Biol.* **77,** 251–290 (2007).
15. Penedo, M. C. *et al.* Microsatellite typing of the rhesus macaque MHC region. *Immunogenetics* **57,** 198–209 (2005).
16. Ferguson, B. *et al.* Single nucleotide polymorphisms (SNPs) distinguish Indian-origin and Chinese-origin rhesus macaques (*Macaca mulatta*). *BMC Genomics* **8,** 43 (2007).
17. Mitalipov, S. *et al.* Isolation and characterization of novel rhesus monkey embryonic stem cell lines. *Stem Cells* **24,** 2177–2186 (2006).
18. Byrne, J. A., Mitalipov, S. M., Clepper, L. & Wolf, D. P. Transcriptional profiling of rhesus monkey embryonic stem cells. *Biol. Reprod.* **75,** 908–915 (2006).
19. Byrne, J. A., Clepper, L., Wolf, D. P. & Mitalipov, S. M. in *International Society for Stem Cell Research, 5th Annual meeting* 52 (Cairns, Queensland, Australia, 2007).
20. Simerly, C. *et al.* Embryogenesis and blastocyst development after somatic cell nuclear transfer in nonhuman primates: overcoming defects caused by meiotic spindle extraction. *Dev. Biol.* **276,** 237–252 (2004).
21. Zhou, Q. *et al.* A comparative approach to somatic cell nuclear transfer in the rhesus monkey. *Hum. Reprod.* **21,** 2564–2571 (2006).
22. Ng, S. C. *et al.* The first cell cycle after transfer of somatic cell nuclei in a non-human primate. *Development* **131,** 2475–2484 (2004).
23. Yang, X. *et al.* Nuclear reprogramming of cloned embryos and its implications for therapeutic cloning. *Nature Genet.* **39,** 295–302 (2007).
24. Munsie, M. J. *et al.* Isolation of pluripotent embryonic stem cells from reprogrammed adult mouse somatic cell nuclei. *Curr. Biol.* **10,** 989–992 (2000).
25. Wakayama, T. *et al.* Differentiation of embryonic stem cell lines generated from adult somatic cells by nuclear transfer. *Science* **292,** 740–743 (2001).
26. Hochedlinger, K. & Jaenisch, R. Monoclonal mice generated by nuclear transfer from mature B and T donor cells. *Nature* **415,** 1035–1038 (2002).
27. Mombaerts, P. Therapeutic cloning in the mouse. *Proc. Natl Acad. Sci. USA* 100, 11924–11925 (2003); published online 29 August 2003.
28. Wakayama, S. *et al.* Equivalency of nuclear transfer-derived embryonic stem cells to those derived from fertilized mouse blastocysts. *Stem Cells* 24, 2023–2033 (2006); published online 11 May 2006.
29. Brambrink, T., Hochedlinger, K., Bell, G. & Jaenisch, R. ES cells derived from cloned and fertilized blastocysts are transcriptionally and functionally indistinguishable. *Proc. Natl Acad. Sci. USA* 103, 933–938 (2006); published online 17 January 2006.
30. Lanza, R. P. *et al.* Generation of histocompatible tissues using nuclear transplantation. *Nature Biotechnol.* 20, 689–696 (2002); published online 3 June 2002.
31. Martin, M. J. *et al.* Skin graft survival in genetically identical cloned pigs. *Cloning Stem Cells* **5,** 117–121 (2003).
32. Yang, J. *et al.* Epigenetic marks in cloned rhesus monkey embryos: comparison with counterparts produced *in vitro*. *Biol. Reprod.* **76,** 36–42 (2007).
33. Wakayama, S. *et al.* Establishment of mouse embryonic stem cell lines from somatic cell nuclei by nuclear transfer into aged, fertilization-failure mouse oocytes. *Curr. Biol.* **17,** R120–R121 (2007).
34. Byrne, J., Mitalipov, S. & Wolf, D. Current progress with primate embryonic stem cells. *Curr. Stem Cell Res. Ther.* **1,** 127–138 (2006).


**Supplementary Information** is linked to the online version of the paper at www.nature.com/nature.

**Acknowledgements** The authors acknowledge the Division of Animal Resources and the Endocrine Services Cores at the Oregon National Primate Research Center for assistance and technical services. We thank M. Sparman, C. Ramsey and V. Dighe of the Assisted Reproductive Technology Core for their embryological and logistical assistance; J. Fanton and D. Jacobs for laparoscopic oocyte retrievals; B. Ferguson for performing the SNP analysis; C. Penedo for microsatellite analysis; and R. Stouffer, M. Grompe and R. Reijo Pera for reviewing this manuscript. Microarray assays were performed in the Affymetrix Microarray Core of the OHSU Gene Microarray Shared Resource. This study was supported by funds from ONPRC and NIH grants to S. Mitalipov, R. Stouffer and D. Dorsa.

**Author Contributions** S.M.M. and J.A.B. designed experiments, conducted SCNT and ES cell derivation. L.L.C. performed DNA/RNA isolations and stemness gene expression. J.A.B. analysed the microarray data and performed the mitochondrial DNA analysis. D.A.P. assisted with ES cell derivation and performed ES cell culture, characterization and differentiation. W.G.S. and M.N. performed the cytogenetic analysis. S.G. analysed teratomas. S.M.M., J.A.B. and D.P.W. analysed the data and wrote the paper.

**Author Information** Microarray data, including CEL and CHP files, and Supplementary Data files containing microarray analyses (Supplementary Data 3–7) have been deposited in the Gene Expression Omnibus (GEO) database with accession number GSE7748 (http://www.ncbi.nlm.nih.gov/geo/query/acc.cgi?acc=GSE7748). Reprints and permissions information is available at www.nature.com/reprints. Correspondence and requests for materials should be addressed to S.M.M. (mitalipo@ohsu.edu).

## METHODS

**Animals.** Adult rhesus macaques housed in individual cages were used in this study. All animal procedures were approved by the Institutional Animal Care and Use Committee at the ONPRC/OHSU

**Ovarian stimulation of rhesus macaques.** Controlled ovarian stimulation and oocyte recovery was performed as has previously been described[35]. Briefly, cycling females were subjected to follicular stimulation using twice-daily intramuscular injections of recombinant human FSH as well as concurrent treatment with Antide, a GnRH antagonist, for days 8–9. Unless indicated otherwise, all reagents were from Sigma-Aldrich and all hormones were from Ares Advanced Technologies Inc. Females received recombinant human luteinizing hormone on days 7-9 and recombinant human chorionic gonadotrophin (hCG) on day 10.

**Somatic cell nuclear transfer.** A primary culture of fibroblasts was established from an adult rhesus macaque male (male 1) as previously described[9]. Briefly, a small skin biopsy was surgically derived, washed in $Ca^{2+}$- and $Mg^{2+}$-free Dulbecco PBS (Invitrogen) and minced into pieces before incubation in Dulbecco Modified Eagle's Medium (DMEM, Invitrogen) containing 1 mg ml$^{-1}$ collagenase IV (Invitrogen) at 37 °C in 5% $CO_2$ for 40 min. Tissue pieces were then vortexed, washed, seeded into 75 cm$^3$ cell culture flasks (Corning) containing DMEM supplemented with 100 IU ml$^{-1}$ penicillin, 100 μg ml$^{-1}$ streptomycin (Invitrogen), 10% FBS (DMEM/FBS culture media) and cultured at 37 °C in 5% $CO_2$ until reaching confluency. Fibroblasts were then disaggregated with trypsin treatment and frozen down in aliquots of $1 \times 10^6$ cells in medium containing 10% dimethyl sulphoxide (DMSO).

Fibroblasts were subsequently thawed, plated onto 4-well dishes (Nunc) and cultured under standard conditions until reaching 50–90% confluency. Cells were then synchronized in the G0/G1 phase of the cell cycle by culturing in DMEM medium with 0.5% FBS for 4 days before SCNT. Cumulus–oocyte complexes were collected from anaesthetized animals by laparoscopic follicular aspiration (28–29 h after hCG) and placed in TALP/HEPES medium[36] (modified Tyrode solution with albumin, lactate and pyruvate) containing 0.3% BSA (TH3) at 37 °C. Oocytes were stripped of cumulus cells by mechanical pipetting after brief exposure (<1 min) to hyaluronidase (0.5 mg ml$^{-1}$) and placed in chemically defined, protein-free HECM-9 medium (hamster embryo culture medium)[37] at 37 °C in 6% $CO_2$, 5% $O_2$ and 89% $N_2$ until further use.

Recipient MII oocytes were transferred to 30 μl manipulation droplets of TH3 with 5 μg ml$^{-1}$ cytochalasin B on a glass bottom manipulation dish (http://www.willcowells.com) covered with paraffin oil (Zander IVF) and incubated at 37 °C for 10–15 min before spindle removal. The chamber was then mounted on an inverted microscope (Olympus) equipped with the Oosight imaging system (CRI, Inc.), glass stage warmer (Tokai Hit, http://www.tokaihit.com) and Narishige micromanipulators. The spindle was located and extracted by aspiration into an enucleation pipette (20–25 μm outer diameter). Metaphase spindle removal was confirmed by its presence in the enucleation pipette. The Oosight imaging system allows non-invasive, polarized light imaging and detection of the spindle based on birefringence. Using this innovative approach, we were able to locate and quickly remove the oocyte spindle real-time with 100% efficiency. After oocyte spindle removal a disaggregated donor somatic cell was aspirated into a micropipette and placed into the perivitelline space of the cytoplast on the side opposite the first polar body. Cell fusion was induced by two 50 μs DC pulses of 2.7 kV cm$^{-1}$ (Electro Square Porator T-820, BTX, Inc.) in 0.25 M D-sorbitol buffer containing 0.1 mM calcium acetate, 0.5 mM magnesium acetate, 0.5 mM HEPES and 1 mg ml$^{-1}$ fatty-acid-free BSA. Successful fusion was confirmed visually 30 min after electroporation by the disappearance of the donor cell in the perivitelline space. All nuclear transfer micromanipulation and fusion procedures were conducted on microscope stage warmers (Tokai Hit) maintaining 37 °C. Reconstructed embryos were activated by exposure to 5 μM ionomycin for 5 min in TALP/HEPES medium supplemented with 1 mg ml$^{-1}$ fatty-acid-free BSA and then transferred for 5 min in TALP/HEPES medium supplemented with 30 mg ml$^{-1}$ fatty-acid-free BSA and 2 mM 6-dimethylaminopurine (DMAP) followed by a 5 h incubation in HECM-9 medium containing 2 mM DMAP at 37 °C in 6% $CO_2$. Activated oocytes were placed in 4-well dishes containing HECM-9 medium supplemented with 10% FBS and 12 μM β-mercaptoethanol (BME) and cultured at 37 °C in 6% $CO_2$, 5% $O_2$ and 89% $N_2$ for a maximum of 10 days with medium change every other day.

**ES cell derivation and culture.** Zonae pellucidae of selected expanded SCNT blastocysts were removed by brief exposure (45–60 s) to 0.5% pronase in TH3 medium. A small proportion of embryos were either transferred directly to MEFs as whole blastocysts or after mechanical dissection of the ICM. Remaining blastocysts were subjected to immunosurgical isolation of the ICMs as previously described[17]. Briefly, zona-free blastocysts were exposed to rabbit anti-rhesus spleen serum (a gift from J. A. Thomson) for 30 min at 37 °C. After extensive washing in TH3, embryos were incubated in guinea-pig complement reconstituted with HECM-9 (1:2, v/v) for an additional 30 min at 37 °C. Partially lysed trophectodermal cells were mechanically dispersed by gentle pipetting with a small bore pipette (125 μm inner diameter; Stripper pipette, Midatlantic Diagnostics Inc.) followed by the rinsing of ICMs three times with TH3 medium. Isolated ICMs were plated onto Nunc 4-well dishes containing mitotically inactivated feeder layers consisting of MEFs and cultured in DMEM/F12 medium with glucose and without sodium pyruvate supplemented with 1% nonessential amino acids, 2 mM L-glutamine, 0.1 mM β-mercaptoethanol and 15% FBS at 37 °C, 3% $CO_2$, 5% $O_2$ and 92% $N_2$. ICMs that attached to the feeder layer and initiated outgrowth were manually dissociated into small cell clumps with a microscalpel and replated onto new MEFs. After the first passage, colonies with ES-cell-like morphology were selected for further propagation, characterization and low-temperature storage as previously described[17]. Medium was changed daily and ES cell colonies were split every 5–7 days by manual dissociation and replating collected clumps onto dishes with fresh MEFs.

***In vitro* and in *vivo* differentiation of ES cells.** For embryoid body formation, entire ES cell colonies were loosely detached from feeder cells and transferred into feeder-free, 6-well, ultra-low adhesion plates (Corning Costar) and cultured in suspension in ES cell medium for 5–7 days. To induce further differentiation, embryoid bodies were transferred into collagen-coated, 6-well culture dishes (Becton Dickinson) to allow attachment. For neuronal differentiation, medium was replaced with serum-free DMEM/F12 containing ITS supplement (insulin, transferrin and sodium selenite, Invitrogen) and fibronectin (5 μg ml$^{-1}$; Invitrogen)[38]. Cultures were maintained for 7 days, with medium replenishment every 2 days. The resulting cultures were disaggregated with collagenase or trypsin treatment and replated onto polyornithine- and laminin-coated plates or glass coverslips in N2 medium consisting of DMEM/F12 supplemented with laminin (1 μg ml$^{-1}$; Invitrogen), bFGF (10 ng ml$^{-1}$; R&D Systems), and N2 supplement (Invitrogen). Cultures were maintained for an additional 7 days with a daily medium change. After 7 days, bFGF was omitted from the medium and cultures were maintained for an additional 7–12 days to induce differentiation into mature neuronal phenotype. Differentiation into cardiac cells was initiated by embryoid body formation in suspension as described above. Embryoid bodies were then plated into collagen-coated dishes and cultures were maintained in ES cell medium for 2–4 weeks. In order to obtain teratomas, 3–5 million undifferentiated ES cells from each cell line were harvested and injected into the hind-leg muscle or subcutaneously into 4-week-old, SCID, beige male mice using an 18 gauge needle. Six to seven weeks after injection, mice were killed and teratomas were dissected, sectioned and histologically characterized for the presence of representative tissues of all three germ layers.

**Immunocytochemical procedures.** Undifferentiated and differentiated ES cells were fixed in 4% paraformaldehyde for 20 min. After permeabilization with 0.2% Triton X-100 and 0.1% Tween-20, nonspecific reactions were blocked with 10% normal serum (Jackson ImmunoResearch Laboratories, Inc.). Cells were then incubated for 40 min in primary antibodies, washed three times and exposed to secondary antibodies conjugated with fluorochromes (Jackson ImmunoResearch) before co-staining with 2 μg ml$^{-1}$ 4',6-diamidino-2-phenylindole (DAPI) for 10 min, whole-mounting onto slides and examination under epifluorescence microscopy. Primary antibodies for OCT4, SSEA-4, TRA1-60 and TRA1-81 were from Santa Cruz Biotechnology Inc. Neural-specific antibodies including microtubule-associated protein (MAP2C), β-III-tubulin and tyrosine hydroxylase were from Chemicon International Inc.

**Cytogenetic analysis.** Mitotically active ES cells in log phase were incubated with 120 ng ml$^{-1}$ ethidium bromide for 40 min at 37 °C, 5% $CO_2$, followed by 120 ng ml$^{-1}$ colcemid (Invitrogen) treatment for 20–40 min. Cells were then dislodged with 0.25% trypsin, and centrifuged at 200*g* for 8 min. The cell pellet was gently re-suspended in 0.075 M KCl solution and incubated for 20 min at 37 °C followed by fixation with methanol:glacial acetic acid (3:1) solution. Cytogenetic analysis was performed on 20 metaphase cells from each ES cell line following standard GTW-banding procedures. Images were acquired using the Cytovision Image Analysis System (Applied Imaging) and karyotypes were arranged as previously described[39]. FISH analysis was performed on metaphase cells from the donor somatic cell line and CRES-1 using BAC CH250-283K14, specific for the rhesus macaque Yq11.21 region. The clone was obtained from the CHORI-250 rhesus macaque BAC library (Children's Hospital Oakland Research Institute, BACPAC Resources), grown in LB media supplemented with 25 μg ml$^{-1}$ chloramphenicol and isolated using a mini-prep protocol adapted from the standard Qiagen plasmid purification method (Qiagen Inc.). Probes were nick-translated with rhodamine-5-dUTP (Enzo Life Sciences) using a modification of the manufacturer's protocol (Vysis). Approximately 200 ng of the probe was precipitated along with 2 μg human Cot-I DNA (Invitrogen). Before hybridization, slides were pre-treated at 73 °C in 2× SSC for 2 min, followed by digestion at 37 °C in a protease solution for 5 min, post-fixation in 10% buffered formaldehyde with 2 M MgCl, and dehydration. The slide and

probe mixture were co-denaturated at 74 °C for 2 min and incubated overnight at 37 °C using the HYBrite system (Vysis). Images were acquired using the Cytovision image analysis system.

**RT–PCR.** Total RNA was extracted from cells using an RNA purification kit (Invitrogen) according to the manufacturer's instructions. Total RNA was treated with DNase I before cDNA preparation using the SuperScript III first-strand synthesis system for RT–PCR (Invitrogen) according to the manufacturer's instructions. The first strand cDNA was further amplified by PCR using individual primer pairs for specific genes. The primer sequence, annealing temperature and amplicon size for each pair of primers are listed in Supplementary Table 5. All PCR samples were analysed by electrophoresis on 2% agarose gel containing 0.5 μg $ml^{-1}$ ethidium bromide and visualized on a transilluminator.

**Microsatellite analysis.** For STR genotyping, DNA was extracted from blood or cultured cells using commercial kits (Gentra). Six multiplexed PCR reactions were set up for the amplification of 39 markers representing 25 autosomal loci and 14 autosomal, MHC-linked loci. On the basis of the published rhesus macaque linkage map[40], these markers are distributed in 19 chromosomes. Two of the markers included in the panel, MFGT21 and MFGT22[41], were developed from *Macaca fuscata* and do not have a chromosome assignment. PCRs were set up in 25 μl reactions containing 30–60 ng DNA, 2.5 mM $MgCl_2$, 200 μM dNTPs, 1× PCR buffer II, 0.5 U Amplitaq (Applied Biosystems) and fluorescence-labelled primers in concentrations ranging from 0.06 to 0.9 μM, as required for each multiplex PCR. Cycling conditions consisted of four cycles of 1 min at 94 °C, 30 s at 58 °C, 30 s at 72 °C, followed by 25 cycles of 45 s at 94 °C, 30 s at 58 °C, 30 s at 72 °C and a final extension at 72 °C for 30 min. PCR products were separated by capillary electrophoresis on the ABI 3730 DNA analyser (Applied Biosystems) according to the manufacturer's instructions. Fragment size analysis and genotyping was done with the computer software STRand (http://www.vgl.ucdavis.edu/informatics/STRand/). Primer sequences for MHC-linked STRs 9P06, 246K06, 162B17(A and B), 151L13, 268P23 and 222I18 were designed from the corresponding rhesus macaque BAC clone sequences deposited in GenBank (accession numbers AC148662, AC148696, AC148683, AC148682, AC148698 and AC148689, respectively). Loci identified by the letter 'D' prefix were amplified using heterologous human primers.

**SNP analysis.** SNP analysis was performed as previously described[16]. Briefly, SNP genotyping was performed using iPLEX reagents and protocols for multiplex PCR, single base primer extension and generation of mass spectra, as per the manufacturer's instructions (for complete details see iPLEX Application Note, Sequenom). Four multiplexed assays containing 56 SNPs were included, 30 which were informative for CRES inheritance (see Supplementary Table 3). All 56 SNPs demonstrated a 100% match between male 1 donor cells and the CRES-1 and CRES-2 cells lines. Initial multiplexed PCRs were performed in 5 μl reactions on 384-well plates containing 5 ng of genomic DNA. Reactions contained 0.5 U HotStar Taq polymerase (QIAGEN), 100 nM primers, 1.25× HotStar Taq buffer, 1.625 mM $MgCl_2$ and 500 μM dNTPs. After enzyme activation at 94 °C for 15 min, DNA was amplified with 45 cycles of 94 °C × 20 s, 56 °C × 30 s, 72 °C × 1 min, followed by a 3-min extension at 72 °C. Unincorporated dNTPs were removed using shrimp alkaline phosphatase (0.3 U, Sequenom). Single-base extension was carried out by addition of single base primer extension primers at concentrations from 0.625 μM to 1.25 μM using iPLEX enzyme and buffers (Sequenom). Single base primer extension products were measured using the MassARRAY Compact system, and mass spectra were analysed using TYPER software (Sequenom).

**Mitochondrial DNA analysis.** DNA was extracted from cell lines using commercial kits (Gentra). The rhesus macaque mitochondrial D-loop hypervariable region 2 (RhDHV2) sequence was amplified for each sample using primers RhDF2 (5′-TAACATATCCGATCAGAGCC-3′) and RhDR (5′-TTAAACACC-CTCTACGCCG-3′)[42]. PCR for each sample was performed using Platinum PCR SuperMix (Invitrogen) containing 0.5 μM of each primer (final volume 50 μl). Reaction conditions were initial denaturation at 94 °C for 2 min; 35 cycles of denaturation at 94 °C for 30 s, annealing at 55 °C for 30 s, extension at 72 °C for 90 s and a final extension at 72 °C for 3 min, generating 544 bp of sequence covering the RhDHV2 region. Products from these reactions were then sequenced to determine polymorphic variation in the RhDHV2 region by direct sequencing. The informative domain 1 (ID1) sequence encompassing *Macaca mulatta* mtDNA nucleotide positions 451–480 (GenBank NC_005943) was identified as containing SNPs informative for the mitochondrial inheritance of both CRES-1 and CRES-2. Each ID1 sequence was confirmed by three other sequencing reactions and all of the RhDHV2 chromatograms used in this project were obtained with Sequencher v. 4.7 (GeneCodes).

**Microarray analysis.** The MIAME (Minimum Information About a Microarray Experiment) guidelines for microarray research[43] were incorporated into the design and implementation of these studies. All the microarray comparison analysis data files cited in the text are available online at the Gene Expression Omnibus (http://www.ncbi.nlm.nih.gov/geo/query/acc.cgi?acc = GSE7748). All the microarray comparison analysis data cited in the text are available at ftp://ftp.ncbi.nih.gov/pub/geo/DATA/supplementary/series/GSE7748. Total RNA was isolated from cell colonies selected for the appropriate ES cell morphology (flat monolayer colony with distinctive cobbled stem cell morphology and a high nucleo-cytoplasmic ratio) using the Invitrogen TRIZOL reagent, followed by further purification with the Qiagen RNeasy MinElute Cleanup Kit. For each cell line examined three biological replicates were used and each replicate represented either a different passage or different sub-line (which had been cultured independently and without mixing for several passages). The RNA samples were quantified using the NanoDrop ND-1000 UV-Vis spectrophotometer (NanoDrop Technologies) and the quality of the RNA was assessed using Lab-on-a-Chip RNA Pico Chips and the 2100 Bioanalyser (Agilent Technologies). Samples with electropherograms that showed a size distribution pattern predictive of acceptable microarray assay performance were considered to be of good quality. Two micrograms of total RNA from each sample were amplified and labelled using a single-cycle cDNA synthesis and an *in vitro* transcription cRNA-RNA labelling system (GeneChip one-cycle target labelling and control reagents; Affymetrix). Following successful cRNA amplification, 10 μg of labelled target cRNA was hybridized to rhesus macaque Genome Arrays (Affymetrix) using standard protocols, as described in the GeneChip Expression Analysis manual (http://www.affymetrix.com/support/technical/manual/expression_manual.affx). The rhesus macaque array contains 52,865 probe sets, representing over 20,000 genes. The arrays were scanned using the GeneChip laser scanner (Affymetrix) and image processing, normalization and expression analysis were performed with the Affymetrix GCOS version 1.4 software. MAS-5 statistical analysis was performed to calculate the signal log ratio (SLR) for each probe set comparison, and the gene expression fold changes between two samples were calculated from the SLR using the following formula: fold change = ($2^{SLR}$). The GCOS 1.4 MAS 5.0 software was used to calculate statistically significant differences in gene expression ($P < 0.002$) between samples.

For the primary microarray comparison analysis (Supplementary Data 3) the $\log_{10}$ of the absolute detected signal for each present 'P' probe set ($P < 0.05$) was plotted in a scatter graph (Supplementary Fig. 8) using Affymetrix GeneChip Operating Software (GCOS) version 1.4. For the correlation value calculations, the microarray data for each individual cell line comparison was filtered to only include probe sets present ($P < 0.05$) in both cell lines. The present probe sets (PP) value details the number of probe sets, post filtering, with a present ($P < 0.05$) signal in both compared cell lines. The correlation value for each cell line comparison was calculated using MAS-5 (Affymetrix microarray suite 5) analysis to calculate the proportion of compared probe sets which demonstrated no significant change 'NC' in gene expression (Supplementary Data 3). Each cell line had three biological replicates and the letter after the cell line name details which replicate was used in the primary microarray comparison analysis.

For the secondary gene-specific analysis, comparison analysis was performed between each of the three control ORMES-10 biological replicates and each of the three somatic donor cell replicates, to give a total of nine somatic–ES cell comparisons (Supplementary Data 4). The following selection criteria were used to identify rhesus somatic-specific genes: (1) genes that were considered to be present ($P < 0.05$) in all three somatic donor cell replicates; and (2) genes that demonstrated statistically significant decrease 'D' in gene expression in the ORMES-10 replicates in all nine comparisons with the somatic donor cell replicates after GCOS comparisons with MAS-5 statistical analysis. A total of 4,998 somatic-specific probe sets were identified in this way (Supplementary Data 5). The following selection criteria were used to identify rhesus ES-cell-specific genes: (1) genes that were considered to be present ($P < 0.05$) in all three ORMES-10 replicates; and (2) genes that demonstrated a statistically significant increase 'I' in gene expression in the ORMES-10 ES cell replicates in all nine comparisons with the somatic donor cell replicates after GCOS comparisons with MAS-5 statistical analysis. A total of 6,178 ES-cell-specific probe sets were identified in this way (Supplementary Data 6). It should be noted that the general approximation when working with large numbers of probe sets is to assume that each probe set represents hybridization to a single gene. However, multiple probe sets can exist for certain genes, so the actual number of genes included in the analysis is significantly lower than the number of probe sets analysed. The somatic-specific and ES-cell-specific genes identified from this comparison analysis were then used to investigate whether the CRES cell lines had successfully downregulated somatic-specific genes (Supplementary Table 4) and successfully upregulated ES-cell-specific genes (Table 2) after comparison analysis with the three somatic donor cell replicates.

For the tertiary stemness gene analysis, stemness genes were derived from our previous transcriptional profiling work with rhesus macaque embryonic stem cell lines[18]. These 12 putative stemness genes had the highest average fold change

in gene expression when three undifferentiated biological replicates of ORMES-6 were compared to their *in vitro* differentiated counterparts, and all 12 were significantly upregulated in five different rhesus macaque embryonic stem cell lines examined[18]. Comparison analysis was performed between the ORMES and CRES cell line replicates and the donor somatic cell replicates (Supplementary Data 7), and the average fold change increase in gene expression of the 12 stemness genes in the ORMES and CRES cell lines was calculated (Table 3). All of the normalized microarray data sets generated from these studies can be found on the GEO website, as noted above.

**Statistical analysis.** Non-microarray results were analysed by chi-squared and unpaired *t*-test using Statview Software (SAS Institute, Inc.) with statistical significance set at 0.05. Microarray results were analysed by MAS-5 statistical analysis in Affymetrix GeneChip Operating Software (GCOS) version 1.4.


35. Zelinski-Wooten, M. B., Hutchison, J. S., Hess, D. L., Wolf, D. P. & Stouffer, R. L. Follicle stimulating hormone alone supports follicle growth and oocyte development in gonadotrophin-releasing hormone antagonist-treated monkeys. *Hum. Reprod.* **10,** 1658–1666 (1995).
36. Bavister, B. D. & Yanagimachi, R. The effects of sperm extracts and energy sources on the motility and acrosome reaction of hamster spermatozoa *in vitro*. *Biol. Reprod.* **16,** 228–237 (1977).
37. McKiernan, S. H. & Bavister, B. D. Culture of one-cell hamster embryos with water soluble vitamins: pantothenate stimulates blastocyst production. *Hum. Reprod.* **15,** 157–164 (2000).
38. Kuo, H. C. *et al.* Differentiation of monkey embryonic stem cells into neural lineages. *Biol. Reprod.* **68,** 1727–1735 (2003).
39. Pearson, P. L. *et al.* Report of the committee on comparative mapping. *Cytogenet. Cell Genet.* **25,** 82–95 (1979).
40. Rogers, J. *et al.* An initial genetic linkage map of the rhesus macaque (*Macaca mulatta*) genome using human microsatellite loci. *Genomics* **87,** 30–38 (2006).
41. Domingo-Roura, X., Lopez-Giraldez, T., Shinohara, M. & Takenaka, O. Hypervariable microsatellite loci in the Japanese macaque (*Macaca fuscata*) conserved in related species. *Am. J. Primatol.* **43,** 357–360 (1997).
42. St John, J. C. & Schatten, G. Paternal mitochondrial DNA transmission during nonhuman primate nuclear transfer. *Genetics* **167,** 897–905 (2004).
43. Brazma, A. *et al.* Minimum information about a microarray experiment (MIAME)—toward standards for microarray data. *Nature Genet.* **29,** 365–371 (2001).